Mathematical and Computer Modelling 49 (2009) 2191–2205

Contents lists available at ScienceDirect

Mathematical and Computer Modelling

journal homepage: www.elsevier.com/locate/mcm

From restoration by topological gradient to medical image segmentation via an asymptotic expansion

Didier Auroux

Institut de Mathématiques de Toulouse, UMR 5219, Université Paul Sabatier Toulouse 3, 31062 Toulouse cedex 9, France

ARTICLE INFO

Article history:
Received 14 February 2008
Accepted 24 July 2008

Keywords:
Topological gradient
Image segmentation
Asymptotic expansion
Image restoration
Edge detection

ABSTRACT

The aim of this article is to present an application of the topological asymptotic expansion to the medical image segmentation problem. We first recall the classical variational of the image restoration problem, and its resolution by topological asymptotic analysis in which the identification of the diffusion coefficient can be seen as an inverse conductivity problem. The conductivity is set either to a small positive coefficient (on the edge set), or to its inverse (elsewhere). In this paper a technique based on a power series expansion of the solution to the image restoration problem with respect to this small coefficient is introduced. By considering the limit when this coefficient goes to zero, we obtain a segmented image, but some numerical issues do not allow a too small coefficient. The idea is to use the series expansion to approximate the asymptotic solution with several solutions corresponding to positive (larger than a threshold) conductivity coefficients via a quadrature formula. We illustrate this approach with some numerical results on medical images.

1. Introduction

In most medical image applications, we can identify mainly two image processing problems, the image restoration and denoising, and the segmentation problem. The presence of noise in the images is for example due to the acquisition process and material, and it is often crucial to denoise the image, see e.g. elastography, in which one needs to compute with a high quality the gradient of the image. The segmentation problem can be seen as a post-processing technique, automatically providing a partition of the image into several parts, and thus increasing the quality of the medical interpretation.

The goal of topological optimization and most image processing problems is to create a partition of a given domain (or set) Ω:

- In topological optimization, we look for the optimal design $\omega \subset \Omega$ and its complement;
- In image processing problems like edge detection, classification, and segmentation, the goal is to split the image into several parts.

For this reason, topological shape optimization and image processing problems have common mathematical methods like level set approaches, material properties optimization, variational methods, etc. In this paper, we will only consider the topological gradient approach that has been introduced for the purpose of topological optimization [37,28,20,3,4,23,22].

More precisely, let Ω be an open bounded domain of $\mathbb{R}^2$ and $j(\Omega) = J(u_\Omega)$ be a cost function to be minimized, where u_Ω is the solution to a given Partial Differential Equation (PDE) problem defined in Ω. For a small $\rho \geq 0$, let $\Omega_\rho = \Omega \setminus \overline{\omega_\rho}$ be the perturbed domain by the insertion of a small hole $\omega_\rho = x_0 + \rho\omega$, where $x_0 \in \Omega$ and ω is a fixed bounded domain

E-mail address: didier.auroux@math.ups-tlse.fr.

0895-7177/$ – see front matter © 2008 Elsevier Ltd. All rights reserved.
doi:10.1016/j.mcm.2008.07.002

containing the origin. The topological sensitivity theory provides an asymptotic expansion of j when ρ tends to zero. It takes the general form

$$j(\Omega_\rho) - j(\Omega) = f(\rho)G(x_0) + \circ(f(\rho)), \tag{1}$$

where $f(\rho)$ is an explicit positive function going to zero with ρ and $G(x_0)$ is called the topological gradient at point x_0. Then to minimize the criterion j, we have to insert small holes at points where G is negative. Using this gradient type information, it is possible to build fast algorithms. In most applications, a satisfying approximation of the optimal solution is reached at the first iteration of the optimization process. A topological sensitivity framework allowing one to obtain such an expansion for general cost functions has been proposed in [20,28,22,23].

The inverse conductivity problem, also known as the Calderon problem [15], consists in identifying the coefficients of a partial differential equation from the knowledge of the Dirichlet to Neumann operator. This problem has been widely studied in the literature [18,19,26,27]. In the particular case of crack identification, the problem seems to be more convenient to solve thanks to the singularities of the solution. Only two measurements are needed to recover several simple cracks [1,9,3]. From the numerical point of view, several methods [5,10,11,13,14,18,31,35] have been proposed, but the topological gradient approach seems to be the most efficient method for crack localization [3].

This crack localization technique has already been adapted to several image processing problems, such as restoration or classification. The idea in all these applications is to consider an image as a piecewise smooth function and its edges can be seen as a set of singularities or cracks. We recall that a classical way to restore an image u from its noisy version v defined in a domain $\Omega \subset \mathbb{R}^2$ is to solve the following PDE problem

$$\begin{cases} -\operatorname{div}(c\nabla u) + u = v & \text{in } \Omega, \\ \partial_n u = 0 & \text{on } \partial\Omega, \end{cases} \tag{2}$$

where c is a small positive constant, ∂_n denotes the normal derivative and n is the outward unit normal to $\partial\Omega$. This method is well known to give poor results: it blurs important structures like edges. In order to improve this method, nonlinear isotropic and anisotropic methods were introduced. We can cite here the work of Perona and Malik [32], Catté et al. [16] and more recently Weickert [40,39] and Aubert [6]. In topological gradient approach, c takes only two values: c_0 in the smooth part of the image and a small value ε on edges or cracks [24,7,8].

The segmentation problem [41,33,29,17] consists in splitting an image into its constituent parts. In the particular case of medical images, the goal is to automatically identify several parts in the image that have different properties (e.g. bones, cancer tissues, etc.). Many approaches have been studied. We can cite here some variational approaches such as the use of the Mumford–Shah functional [30], or active contours and snakes [12,36,33,42,38]. The idea of this paper is to consider the same PDE as in restoration problems, but with $c = \varepsilon$ or $\frac{1}{\varepsilon}$, where $\varepsilon > 0$ and $\varepsilon \to 0$. We first propose studying the asymptotic expansion of the solution u_ε of the corresponding PDE with respect to ε. If we assume that $u_0 := \lim_{\varepsilon\to 0} u_\varepsilon$ exists, then u_0 can be seen as a segmentation of the original image v.

This article is organized as follows. In Section 2, we recall the topological asymptotic expansion theory, applied to the image restoration problem. In Section 3, we consider the segmentation problem, based on the same PDE but with different coefficients. We then point out the numerical issues when $\varepsilon \to 0$ and we present an efficient way to compute the segmented image. Then we present various numerical results at the end of Section 3. We end the paper with some concluding remarks in Section 4.

2. Image restoration by topological asymptotic analysis

2.1. Introduction to topological asymptotic analysis

Let Ω be an open bounded domain of $\mathbb{R}^2$ (note that it can be extended easily to $\mathbb{R}^n$). We consider a partial differential equation problem defined in Ω, and we denote by u_Ω its solution (we will further see under which assumptions it can be considered). We finally consider a cost function $J(\Omega, u_\Omega)$ to be minimized, where u_Ω is the solution to the PDE in Ω. The idea of topological asymptotic analysis is to measure the impact of a perturbation of the domain Ω on the cost function. For a small $\rho \geq 0$, let $\Omega_\rho = \Omega \setminus \sigma_\rho$ be the perturbed domain by the insertion of a crack $\sigma_\rho = x_0 + \rho\sigma(n)$, where $x_0 \in \Omega$, $\sigma(n)$ is a straight crack, and n a unit vector normal to the crack. The topological gradient theory can also be applied in the case of arbitrary shaped holes [2,20,22,23], but we will only consider the case of crack perturbations in our applications. The small parameter ρ will represent the size of the inserted crack. Finally, we denote by $\mathcal{V}$ a Hilbert space on Ω, usually $H^1(\Omega)$ in our applications.

We now consider the variational formulation of the PDE problem on Ω

$$\begin{cases} \text{Find } u \in \mathcal{V} \text{ such that} \\ a(u, w) = l(w), \quad \forall w \in \mathcal{V}, \end{cases} \tag{3}$$

and the corresponding variational formulation of the PDE problem on the perturbed domain

$$\begin{cases} \text{Find } u_\rho \in \mathcal{V}_\rho \text{ so that} \\ a_\rho(u_\rho, w) = l_\rho(w), \quad \forall w \in \mathcal{V}_\rho. \end{cases} \tag{4}$$

One should notice that for $\rho = 0$, the perturbed PDE problem becomes the original PDE problem.

We assume in the following that a_ρ is a bilinear continuous and coercive form defined on $\mathcal{V}_\rho$, a Hilbert space on Ω_ρ, and that l_ρ is a linear continuous form on $\mathcal{V}_\rho$.

We can rewrite the cost function J as a function of ρ by considering the following map

$$j : \rho \mapsto \Omega_\rho \mapsto u_\rho \text{solution to problem (4)} \mapsto j(\rho) := J(\Omega_\rho, u_\rho). \tag{5}$$

In order to apply the topological asymptotic theory, a_ρ, l_ρ and J have to satisfy the hypotheses of the following theorem [34,3].

Theorem 1. *If there exist a linear form L_ρ defined on $\mathcal{V}_\rho$, a function $f : \mathbb{R}^+ \to \mathbb{R}^+$, and four real numbers δJ_1, δJ_2, δa and δl so that:*

1. $\lim_{\rho\to 0} f(\rho) = 0$,
2. $J_{\Omega_\rho}(u_\rho) - J_{\Omega_\rho}(u_0) = L_\rho(u_\rho - u_0) + f(\rho)\delta J_1 + o(f(\rho))$,
3. $J_{\Omega_\rho}(u_0) - J_{\Omega}(u_0) = f(\rho)\delta J_2 + o(f(\rho))$,
4. $(a_\rho - a_0)(u_0, p_\rho) = f(\rho)\delta a + o(f(\rho))$,
5. $(l_\rho - l_0)(p_\rho) = f(\rho)\delta l + o(f(\rho))$,

where the adjoint state p_ρ is the solution of the adjoint equation

$$a_\rho(w, p_\rho) = -L_\rho(w) \quad \forall w \in \mathcal{V}_\rho, \tag{6}$$

and u_ρ is the solution of the direct equation

$$a_\rho(u_\rho, w) = l_\rho(w) \quad \forall w \in \mathcal{V}_\rho. \tag{7}$$

Then the cost function has the following asymptotic expansion

$$j(\rho) - j(0) = f(\rho)g(x) + o\left(f(\rho)\right), \tag{8}$$

where $g(x)$ is the topological gradient, given by

$$g(x) = \delta J_1 + \delta J_2 + \delta a - \delta l. \tag{9}$$

Then, from an asymptotic point of view, as $f(\rho) \geq 0$, the idea is to create cracks in the domain Ω where the topological gradient g is the most negative, because

$$J(\Omega_\rho, u_\rho) = J(\Omega, u) + f(\rho)g(x) + o\left(f(\rho)\right) \tag{10}$$

and the cost function corresponding to the perturbed problem will be smaller than the original one. The main advantage of this method is that it only requires the resolution of the direct (4) and adjoint (6) problems.

2.2. Application to image restoration

In this section, we use the topological gradient as a tool for detecting edges for image restoration.

2.2.1. Variational formulation and topological gradient

Let Ω be an open bounded domain of $\mathbb{R}^2$. For v a given function in $L^2(\Omega)$, the initial problem is defined on the safe domain and reads as follows: find $u \in H^1(\Omega)$ such that

$$\begin{cases} -\text{div}\,(c\nabla u) + u = v & \text{in } \Omega, \\ \partial_n u = 0 & \text{on } \partial\Omega, \end{cases} \tag{11}$$

where n denotes the outward unit normal to $\partial\Omega$ and c is a constant function.

For a given $x_0 \in \Omega$ and a small $\rho \geq 0$, let us now consider $\Omega_\rho = \Omega \setminus \overline{\sigma_\rho}$ the perturbed domain by the insertion of a crack $\sigma_\rho = x_0 + \rho\sigma(n)$, where $x_0 \in \Omega$, $\sigma(n)$ is a straight crack, and n a unit vector normal to the crack. Then, the new solution $u_\rho \in H^1(\Omega_\rho)$ satisfies

$$\begin{cases} -\text{div}\left(c\nabla u_\rho\right) + u_\rho = v & \text{in } \Omega_\rho, \\ \partial_n u_\rho = 0 & \text{on } \partial\Omega_\rho. \end{cases} \tag{12}$$

Problem (12) can be rewritten as

$$\begin{cases} \text{Find } u_\rho \in H^1(\Omega_\rho) \text{ such that} \\ a_\rho(u_\rho, w) = l_\rho(w) \quad \forall w \in H^1(\Omega_\rho), \end{cases} \tag{13}$$

where a_ρ is the following bilinear form, defined on $H^1(\Omega_\rho)$ by

$$a_\rho(u, w) = \int_{\Omega_\rho} (c\nabla u\nabla w + uw)\,\mathrm{d}x, \tag{14}$$

and l_ρ is the linear form defined on $L^2(\Omega_\rho)$ by

$$l_\rho(w) = \int_{\Omega_\rho} vw\mathrm{d}x. \tag{15}$$

Edge detection is equivalent to looking for a subdomain of Ω where the energy is small. So our goal is to minimize the energy norm outside edges

$$j(\rho) = J_\rho(u_\rho) = \int_{\Omega_\rho} \|\nabla u_\rho\|^2. \tag{16}$$

To study the asymptotic behaviour when ρ tends to zero of the criterion $j(\rho) = J_\rho(u_\rho)$, and in order to apply the topological asymptotic theory, we suppose that there exist a function $f : \mathbb{R}^+ \to \mathbb{R}^+$ going to zero with ρ, a linear form L_ρ, and four real numbers δJ_1, δJ_2, δa and δl such that the following assumptions are satisfied:

1. $J_\rho\left(u_\rho\right) - J_\rho(u_0) = L_\rho(u_\rho - u_0) + f(\rho)\delta J_1 + o(f(\rho))$,
2. $J_\rho\left(u_0\right) - J_0(u_0) = f(\rho)\delta J_2 + o(f(\rho))$,
3. $\left(a_\rho - a_0\right)\left(u_0, p_\rho\right) = f(\rho)\delta a + o(f(\rho))$,
4. $\left(l_\rho - l_0\right)\left(p_\rho\right) = f(\rho)\delta l + o(f(\rho))$,

where p_ρ is the solution to the adjoint problem

$$a_\rho(w, p_\rho) = -L_\rho(w) \quad \forall w \in H^1(\Omega_\rho). \tag{17}$$

The solution p_ρ is only used for the theoretical analysis, but numerically we just consider the function p_0 the adjoint state, which is independent of the location of the crack.

For our restoration problem, the previous hypotheses are satisfied, and the asymptotic expansion of $j(\rho)$ is given by

$$j(\rho) = j(0) + f(\rho)(\delta a - \delta l + \delta J_1 + \delta J_2) + o(f(\rho)). \tag{18}$$

In our case, the cost function j has the following asymptotic expansion [25]

$$j(\rho) - j(0) = \rho^2 G(x_0, n) + o(\rho^2), \tag{19}$$

with

$$G(x_0, n) = -\pi c(\nabla u_0(x_0).n)(\nabla p_0(x_0).n) - \pi|\nabla u_0(x_0).n|^2. \tag{20}$$

and where p_0 is the solution to the adjoint problem

$$\begin{cases} -\mathrm{div}(c\nabla p_0) + p_0 = -\partial_u J(u) & \text{in } \Omega, \\ \partial_n p_0 = 0 & \text{on } \partial\Omega. \end{cases} \tag{21}$$

The topological gradient could be written as

$$G(x, n) = \langle M(x)n, n\rangle, \tag{22}$$

where $M(x)$ is the 2×2 symmetric matrix defined by

$$M(x) = -\pi c\frac{\nabla u_0(x)\nabla p_0(x)^{\mathrm{T}} + \nabla p_0(x)\nabla u_0(x)^{\mathrm{T}}}{2} - \pi\nabla u_0(x)\nabla u_0(x)^{\mathrm{T}}. \tag{23}$$

For a given x, $G(x, n)$ takes its minimal value when n is the eigenvector associated to the lowest eigenvalue $\lambda_{\min}$ of M. This value will be considered as the topological gradient associated to the optimal orientation of the crack $\sigma_\rho(n)$.

2.2.2. Algorithm

Our algorithm consists in inserting small heterogeneities in regions where the topological gradient is smaller than a given threshold $\alpha < 0$. These regions are the edges of the image. The algorithm is as follows.

Restoration algorithm:

- Initialization : $c = c_0$.
- Calculation of u_0 and p_0: solutions of the direct (11) and adjoint (21) problems.
- Computation of the 2×2 matrix M and its lowest eigenvalue $\lambda_{\min}$ at each point of the domain.
- Set

$$c_1 = \begin{cases} \varepsilon \text{ if } x \in \Omega \text{ such that } \lambda_{\min} < \alpha < 0, \quad \varepsilon > 0 \\ c_0 \quad \text{elsewhere.} \end{cases} \tag{24}$$

- Calculation of u_1 solution to problem (12) using c_1.

From the numerical point of view, it is more convenient to simulate the cracks by a small value of c. The solution u_1 is the restored image.

As in the previous section (inpainting problems), our algorithm requires only 3 resolutions of a partial differential equations in the domain Ω: the direct and adjoint original problems, and then the direct perturbed problem. The complexity of this algorithm is still $\mathcal{O}(n.\log(n))$, where n is the number of pixels of the image, because we can use, as in the previous section, a DCT (discrete cosine transform) for the resolution of the first two problems, and then the DCT solver is used as a preconditioner to the PCG (preconditioned conjugate gradient) algorithm. See [7,8] for more details.

The restoration algorithm for color images is almost the same. For reasons of simplicity, one can simply decompose the color image v in its channels: $v = (v^1, v^2, v^3)$ where v^i represents the intensity of the channel i. For instance, if we decompose the color image in the RGB (red, green, blue) space, v^1 will represent the intensity of red. Then, it is easy to solve Eqs. (12) and (21) separately. But one can also solve directly this equation with vectorial images u and p. The topological gradient is still given by equalities (22) and (23), where all the involved functions are vectorial (it is simply the sum of these expressions for the three channels). One can finally solve separately the three perturbed direct problems, and recompose the restored image u_1, or solve directly the perturbed problem in a vectorial approach.

2.3. Numerical results

The goal of the following numerical results is to prove that the topological gradient method is able to denoise an image and preserve features such as edges.

Fig. 1 shows the restoration algorithm applied to a 256×256 medical image, in grey level. The noisy image is obtained with an additive Gaussian noise, with a signal to noise ratio (SNR) equal to 10.5. This noise can simulate, in a first approximation, the acquisition errors. The identified edges correspond to the pixels where the most negative eigenvalue of the matrix M is smaller than a given threshold. Finally, the last image corresponds to the restored image. The SNR of the restored image is 17.3, and the edges are very well preserved, even if the original level of noise was quite high.

Fig. 2 shows the same restoration process, but with a different grey scale (only for displaying, not for the restoration process) in order to have a better view of the image.

In order to see more clearly the noise reduction in this process, Fig. 3 shows the difference between the original and noisy images (i.e. the additive noise we added to the original image), and the error distribution after the restoration process (i.e. the difference between the original and restored images). One can see that the error is strongly reduced. One can also notice that part of the restoration error is still located on the contours, even if they are very well preserved by the process.

3. Application to medical image segmentation

This section is concerned with image segmentation, the aim of which is to find a partition of an image into its constituent parts. Several variational approaches have been studied for general images, for example the Mumford–Shah functional [30] and the active contours [12,36]. The idea is to apply our topological gradient based algorithm for the detection of edges in the image. We have already seen that the segmentation consists in splitting the image into several parts with a nearly constant criterion (e.g. the grey level from a general imaging point of view, or the tissue conductivity from a more specific medical point of view). This can largely improve the image interpretation.

3.1. From restoration to segmentation

We still consider the restoration equation, and we denote by $u_\varepsilon \in H^1(\Omega)$ the solution to the following problem

$$\begin{cases} -\text{div}\,(c(\varepsilon)\nabla u_\varepsilon) + u_\varepsilon = v & \text{in } \Omega, \\ \partial_n u_\varepsilon = 0 & \text{on } \partial\Omega, \end{cases} \tag{25}$$

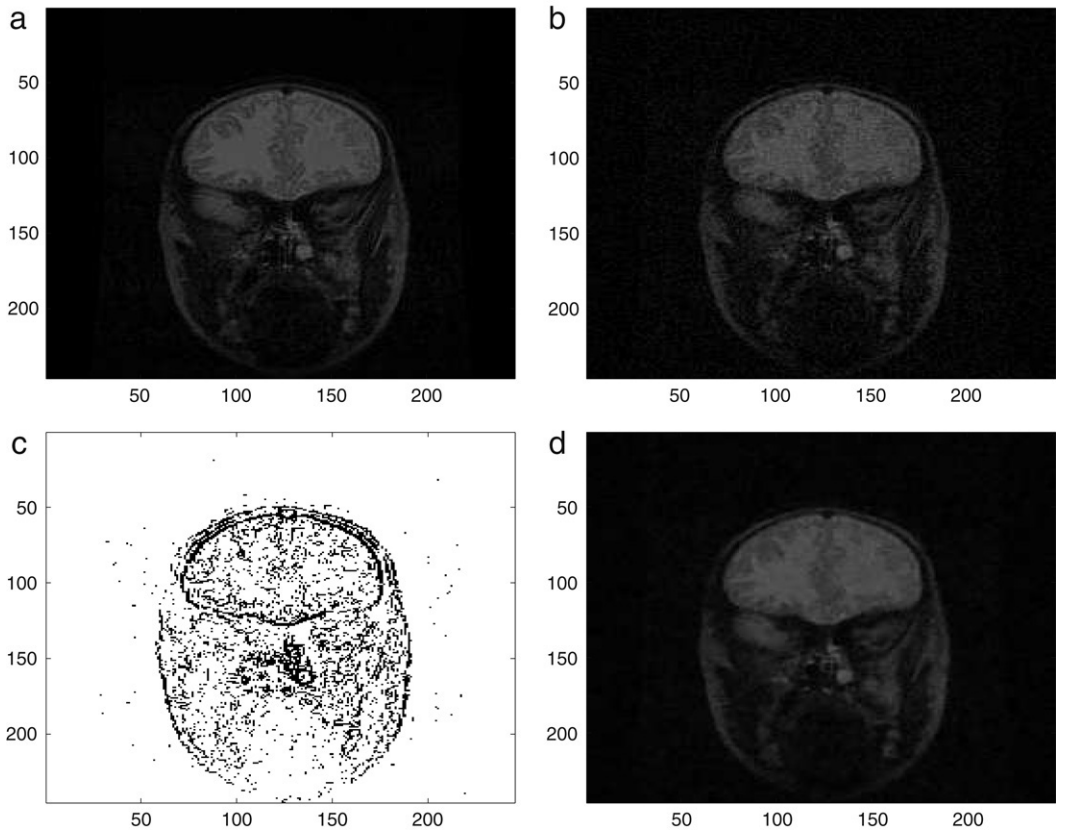

Fig. 1. Restoration of a medical image: initial image (256 × 256 pixels) (a); noisy image (SNR = 10.5) (b); identified edges by the topological gradient (c); restored image using the restoration algorithm (SNR = 17.3) (d).

where $v \in L^2(\Omega)$ is the original image, and $c(\varepsilon)$ is defined by

$$c(\varepsilon) = \begin{cases} \varepsilon & \text{on the edge set,} \\ \dfrac{1}{\varepsilon} & \text{elsewhere.} \end{cases} \tag{26}$$

We will further denote by $\omega \subset \Omega$ the edge set, and assume it is thickened (i.e. of codimension 0 in Ω). Problem (25) can be rewritten as follows

$$(\mathcal{P}_\varepsilon) \begin{cases} -\operatorname{div}(\varepsilon \nabla u_\varepsilon) + u_\varepsilon = v & \text{in } \omega, \\ -\operatorname{div}\left(\dfrac{1}{\varepsilon}\nabla u_\varepsilon\right) + u_\varepsilon = v & \text{in } \Omega \setminus \omega, \\ \partial_n u_\varepsilon = 0 & \text{on } \partial\Omega, \end{cases} \tag{27}$$

where $u_\varepsilon \in H^1(\Omega)$, i.e. with the implicit boundary condition that $c(\varepsilon)\partial_n u_\varepsilon$ has the same value on both sides of $\partial\omega$. We have the following result, when $\varepsilon \to 0$:

Theorem 2. *If we denote by u_ε the unique solution of problem $(\mathcal{P}_\varepsilon)$ in $H^1(\Omega)$, then*

$$\lim_{\varepsilon \to 0} \left(\|\nabla u_\varepsilon - \nabla u_0\|_{L^2(\Omega\setminus\omega)} + \|u_\varepsilon - u_0\|_{L^2(\omega)} \right) = 0, \tag{28}$$

where $u_0 \in H^1(\Omega \setminus \omega) \cap L^2(\Omega)$ is the solution to the following problem

$$(\mathcal{P}_0) \begin{cases} u_0 = v & \text{in } \omega, \\ -\operatorname{div}(\nabla u_0) = 0 & \text{in } \Omega \setminus \omega, \\ \partial_n u_0 = 0 & \text{on } \partial\omega, \\ \partial_n u_0 = 0 & \text{on } \partial\Omega. \end{cases} \tag{29}$$

In order to prove this result, we first need the following lemma:

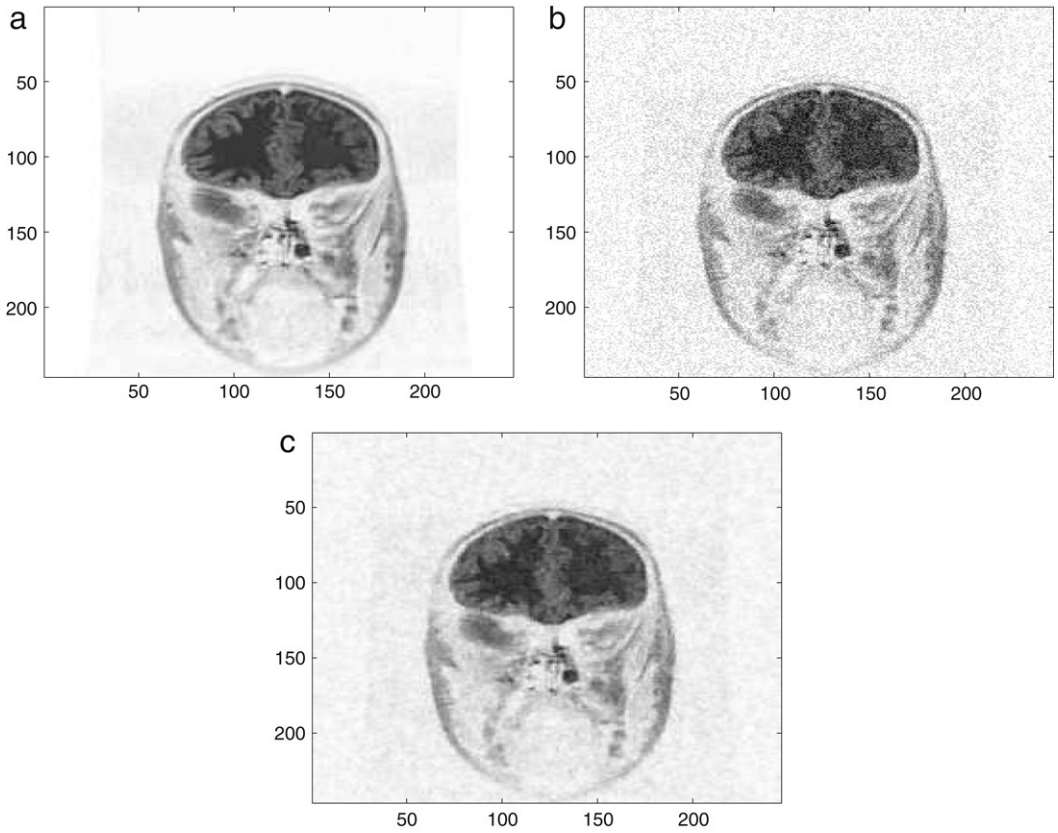

Fig. 2. Restoration of a medical image using a different scale for the display: original image (a); noisy image (SNR = 10.5) (b); restored image using the restoration algorithm (SNR = 17.3) (c).

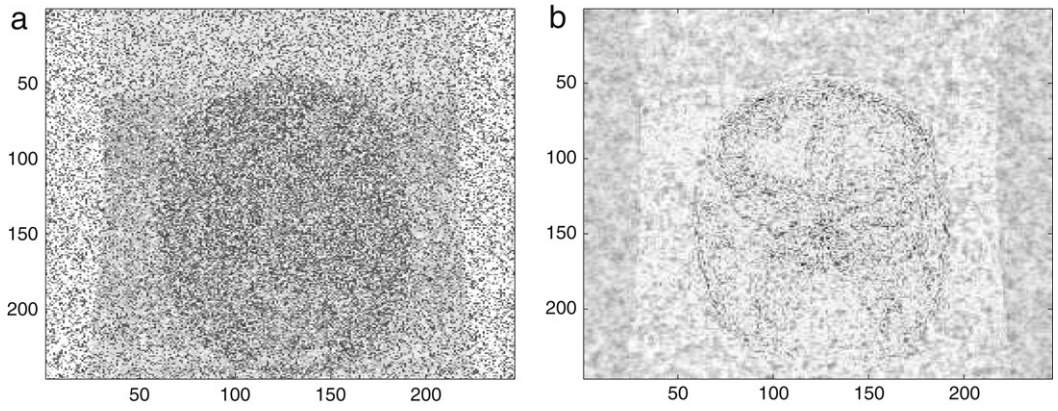

Fig. 3. Restoration of a medical image: difference between the original and noisy images (a); difference between the original and restored images using the same scale (b).

Lemma 1. *The solution u_ε is bounded in $H^1(\Omega)$ by the $L^2(\Omega)$ norm of v:*

$$\|u_\varepsilon\|_{L^2(\Omega)} \leq \|v\|_{L^2(\Omega)}, \tag{30}$$

$$\|\nabla u_\varepsilon\|_{L^2(\omega)} \leq \frac{1}{\sqrt{\varepsilon}}\|v\|_{L^2(\Omega)}, \quad \|\nabla u_\varepsilon\|_{L^2(\Omega\setminus\omega)} \leq \sqrt{\varepsilon}\|v\|_{L^2(\Omega)}. \tag{31}$$

Proof. We consider the variational formulation of problem $(\mathcal{P}_\varepsilon)$, using u_ε as a test function:

$$\int_{\Omega\setminus\omega} \frac{1}{\varepsilon}\nabla u_\varepsilon \nabla u_\varepsilon + \int_\omega \varepsilon \nabla u_\varepsilon \nabla u_\varepsilon + \int_\Omega u_\varepsilon u_\varepsilon = \int_\Omega v u_\varepsilon,$$

which gives

$$\frac{1}{\varepsilon}\|\nabla u_\varepsilon\|^2_{L^2(\Omega\setminus\omega)} + \varepsilon\|\nabla u_\varepsilon\|^2_{L^2(\omega)} + \|u_\varepsilon\|^2_{L^2(\Omega)} = \int_\Omega v u_\varepsilon \le \|v\|_{L^2(\Omega)}\|u_\varepsilon\|_{L^2(\Omega)}.$$

We have then

$$\|u_\varepsilon\|^2_{L^2(\Omega)} \le \|v\|_{L^2(\Omega)}\|u_\varepsilon\|_{L^2(\Omega)},$$

which gives the L^2 bound of u_ε. Then, we have

$$\frac{1}{\varepsilon}\|\nabla u_\varepsilon\|^2_{L^2(\Omega\setminus\omega)} + \varepsilon\|\nabla u_\varepsilon\|^2_{L^2(\omega)} \le \|v\|_{L^2(\Omega)}\|u_\varepsilon\|_{L^2(\Omega)} \le \|v\|^2_{L^2(\Omega)},$$

and then Eq. (31) follows. □

We can now give a proof of Theorem 2:

Proof. The corresponding variational formulation of problem $(\mathcal{P}_\varepsilon)$ is

$$\int_{\Omega\setminus\omega} \frac{1}{\varepsilon}\nabla u_\varepsilon \nabla \phi + \int_\omega \varepsilon \nabla u_\varepsilon \nabla \phi + \int_\Omega u_\varepsilon \phi = \int_\Omega v\phi, \quad \forall \phi \in H^1_0(\Omega).$$

We first choose $\phi = \phi_1$ as test functions, where $\phi_1 \in H^1_0(\Omega \setminus \omega)$. The variational formulation becomes

$$\int_{\Omega\setminus\omega} \frac{1}{\varepsilon}\nabla u_\varepsilon \nabla \phi_1 + \int_{\Omega\setminus\omega} (u_\varepsilon - v)\phi_1 = 0, \quad \forall \phi_1 \in H^1_0(\Omega \setminus \omega).$$

By multiplying all the terms of the equation by ε, we obtain

$$\int_{\Omega\setminus\omega} \nabla u_\varepsilon \nabla \phi_1 + \int_{\Omega\setminus\omega} \varepsilon(u_\varepsilon - v)\phi_1 = 0, \quad \forall \phi_1 \in H^1_0(\Omega \setminus \omega).$$

We consider the same kind of test function in the variational formulation of problem $(\mathcal{P}_0)$ and we obtain:

$$\int_{\Omega\setminus\omega} \nabla u_0 \nabla \phi_1 = 0, \quad \forall \phi_1 \in H^1_0(\Omega \setminus \omega).$$

The subtraction between these two previous equations gives

$$\int_{\Omega\setminus\omega} \nabla(u_\varepsilon - u_0)\nabla \phi_1 = -\varepsilon \int_{\Omega\setminus\omega} (u_\varepsilon - v)\phi_1, \quad \forall \phi_1 \in H^1_0(\Omega \setminus \omega).$$

By using Lemma 1 when $\varepsilon \to 0$, as u_ε has a bounded L^2 norm, independently of ε, then the right-hand side goes to 0 with ε, and we obtain

$$\lim_{\varepsilon\to 0} \|\nabla u_\varepsilon - \nabla u_0\|_{L^2(\Omega\setminus\omega)} = 0.$$

From a similar way, by using $\phi = \phi_2$ as test functions, where $\phi_2 \in H^1_0(\omega)$, the previous variational formulation becomes

$$\int_\omega \varepsilon \nabla u_\varepsilon \nabla \phi_2 + \int_\omega (u_\varepsilon - v)\phi_2 = 0, \quad \forall \phi_2 \in H^1_0(\omega).$$

The corresponding variational formulation of problem $(\mathcal{P}_0)$ is

$$\int_\omega (u_0 - v)\phi_2 = 0, \quad \forall \phi_2 \in H^1_0(\omega),$$

and the subtraction between these two previous equations gives

$$\int_\omega (u_\varepsilon - u_0)\phi_2 = -\varepsilon \int_\omega \nabla u_\varepsilon \nabla \phi_2, \quad \forall \phi_2 \in H^1_0(\omega).$$

By using Lemma 1 when $\varepsilon \to 0$, as $\varepsilon\|\nabla u_\varepsilon\|_{L^2(\omega)} \le \sqrt{\varepsilon}\|v\|_{L^2(\Omega)}$, then the right-hand side goes to 0 with ε, and we obtain

$$\lim_{\varepsilon\to 0} \|u_\varepsilon - u_0\|_{L^2(\omega)} = 0. \quad \square$$

3.2. Approximation on the edge set

We will now assume that the edge set ω is of codimension 1 in Ω. From the point of view of applications, it is completely natural to assume that the edges are *flat* in the image. In order to have coherent notations, we will further denote by σ the edge set.

We can rewrite our approximated segmentation problem $(\mathcal{P}_\varepsilon)$ as follows

$$(\tilde{\mathcal{P}}_\varepsilon)\begin{cases} -\mathrm{div}\left(\frac{1}{\varepsilon}\nabla u_\varepsilon\right) + u_\varepsilon = v & \text{in } \Omega \setminus \sigma, \\ \partial_n u_\varepsilon = 0 & \text{on } \sigma, \\ \partial_n u_\varepsilon = 0 & \text{on } \partial\Omega, \end{cases} \tag{32}$$

where $u_\varepsilon \in H^1(\Omega \setminus \sigma)$. If $v \in L^2(\Omega)$, then problem $(\tilde{\mathcal{P}}_\varepsilon)$ has a unique solution in $H^1(\Omega \setminus \sigma)$. As a corollary of the previous results, we have the following one:

Theorem 3. *If we denote by u_ε the unique solution of problem $(\tilde{\mathcal{P}}_\varepsilon)$ in $H^1(\Omega \setminus \sigma)$, then*

$$\begin{aligned} &\|u_\varepsilon\|_{L^2(\Omega)} \leq \|v\|_{L^2(\Omega)}, \\ &\|\nabla u_\varepsilon\|_{L^2(\Omega\setminus\sigma)} \leq \sqrt{\varepsilon}\|v\|_{L^2(\Omega)}, \end{aligned} \tag{33}$$

and

$$\lim_{\varepsilon\to 0} \|\nabla u_\varepsilon - \nabla u_0\|_{L^2(\Omega\setminus\sigma)} = 0 \tag{34}$$

where $u_0 \in H^1(\Omega \setminus \sigma)$ is the unique solution to the following problem

$$(\tilde{\mathcal{P}}_0)\begin{cases} -\mathrm{div}(\nabla u_0) = 0 & \textit{in } \Omega \setminus \sigma, \\ \displaystyle\int_{\Omega_i} u_0 = \int_{\Omega_i} v & \forall \Omega_i \textit{ connex component of } \Omega \setminus \sigma, \\ \partial_n u_0 = 0 & \textit{on } \sigma, \\ \partial_n u_0 = 0 & \textit{on } \partial\Omega. \end{cases} \tag{35}$$

Proof. This result follows from the previous theorem. The only different point is the second equation in problem $(\tilde{\mathcal{P}}_0)$. As u_0 is the solution of the Poisson problem with a homogeneous Neumann boundary condition, we need an additional equation to close the system. This condition can be easily deduced from the variational formulation of problem $(\tilde{\mathcal{P}}_\varepsilon)$, using $\phi = \chi_{\Omega_i}$ as a test function, where Ω_i is a connex component of $\Omega \setminus \sigma$. □

For numerical reasons, it can be very difficult to solve directly problem $(\tilde{\mathcal{P}}_0)$, and even problem $(\tilde{\mathcal{P}}_\varepsilon)$ for too small values of $\varepsilon > 0$. The conditioning of the system to be solved goes to infinity when $\varepsilon \to 0$. For example, the conditioning of the 2D discrete Laplacian is $\frac{1+\cos\left(\frac{\pi}{n+1}\right)}{1-\cos\left(\frac{\pi}{n+1}\right)}$, where n is the number of discretization points (i.e. the number of pixels in the image). This conditioning goes to infinity with n, and for example, if $n = 10^6$, it is larger than 10^{11}.

But the main issue arises from the fact that the second equation in problem $(\tilde{\mathcal{P}}_0)$ cannot usually be directly implemented in a numerical scheme. Moreover, $\Omega \setminus \omega$ might have only one connex component if the edge set is not precisely computed or if some edge points are missing, as can be seen in Fig. 1, and a direct resolution with this mean condition would give a constant function over all $\Omega \setminus \sigma$.

3.3. Series expansion

In order to overcome this issue, we will expand the solution u_ε of problem $(\tilde{\mathcal{P}}_\varepsilon)$ into a power series of ε [21]. From the knowledge of this power series expansion and the computation of several solutions u_ε for not too small coefficients $\varepsilon > 0$, it will be possible to approximate the asymptotic solution u_0. We have the following result.

Theorem 4. *There exist a constant $\varepsilon_c > 0$ and a family of functions $(u_n)_{n\in\mathbb{N}}$ of $H^1(\Omega \setminus \sigma)$ such that, for all $0 \leq \varepsilon < \varepsilon_c$,*

$$u_\varepsilon = \sum_{n=0}^{\infty} u_n \varepsilon^n. \tag{36}$$

Moreover, these functions (u_n) are the unique solutions in $H^1(\Omega \setminus \sigma)$ of the following problems:

$$(\tilde{\mathcal{P}}_0)\begin{cases} -\mathrm{div}(\nabla u_0) = 0 & \text{in } \Omega \setminus \sigma, \\ \displaystyle\int_{\Omega_i} u_0 = \int_{\Omega_i} v & \forall \Omega_i \text{ connex component of } \Omega \setminus \sigma, \\ \partial_n u_0 = 0 & \text{on } \sigma, \\ \partial_n u_0 = 0 & \text{on } \partial\Omega. \end{cases} \tag{37}$$

$$(\tilde{\mathcal{P}}_1)\begin{cases} -\mathrm{div}(\nabla u_1) = -u_0 + v & \text{in } \Omega \setminus \sigma, \\ \displaystyle\int_{\Omega_i} u_1 = 0 & \forall \Omega_i \text{ connex component of } \Omega \setminus \sigma, \\ \partial_n u_1 = 0 & \text{on } \sigma, \\ \partial_n u_1 = 0 & \text{on } \partial\Omega, \end{cases} \tag{38}$$

and for $n \geq 2$,

$$(\tilde{\mathcal{P}}_n)\begin{cases} -\mathrm{div}(\nabla u_n) = -u_{n-1} & \text{in } \Omega \setminus \sigma, \\ \displaystyle\int_{\Omega_i} u_n = 0 & \forall \Omega_i \text{ connex component of } \Omega \setminus \sigma, \\ \partial_n u_n = 0 & \text{on } \sigma, \\ \partial_n u_n = 0 & \text{on } \partial\Omega. \end{cases} \tag{39}$$

Proof. It is straightforward to see that problem $(\tilde{\mathcal{P}}_n)$ has a unique solution $u_n \in H^1(\Omega \setminus \sigma)$, for all $n \geq 0$. The variational formulation of problem $(\tilde{\mathcal{P}}_n)$ gives, using u_n as a test function and for $n \geq 2$,

$$\|\nabla u_n\|^2_{L^2(\Omega\setminus\sigma)} = -\int_{\Omega\setminus\sigma} u_n u_{n-1} \leq \|u_n\|_{L^2(\Omega)} \|u_{n-1}\|_{L^2(\Omega)}.$$

By using the Poincaré inequality on $\Omega \setminus \sigma$, if we denote by $C_1 > 0$ the corresponding constant, as the mean of u_n over each connex component of $\Omega \setminus \sigma$ is equal to zero, we have

$$\|u_n - 0\|^2_{L^2(\Omega\setminus\sigma)} \leq C_1^2 \|\nabla u_n\|^2_{L^2(\Omega\setminus\sigma)} \leq C_1^2 \|u_n\|_{L^2(\Omega)} \|u_{n-1}\|_{L^2(\Omega)},$$

and then

$$\|u_n\|_{L^2(\Omega)} \leq C_1^2 \|u_{n-1}\|_{L^2(\Omega)}. \tag{40}$$

We also have

$$\|\nabla u_n\|^2_{L^2(\Omega\setminus\sigma)} \leq \|u_n\|_{L^2(\Omega)} \|u_{n-1}\|_{L^2(\Omega)} \leq C_1^2 \|u_{n-1}\|^2_{L^2(\Omega)}$$

and then

$$\|\nabla u_n\|_{L^2(\Omega\setminus\sigma)} \leq C_1 \|u_{n-1}\|_{L^2(\Omega)}. \tag{41}$$

This implies that the following power series

$$\sum_{n=0}^{\infty} u_n \varepsilon^n \quad \text{and} \quad \sum_{n=0}^{\infty} \nabla u_n \varepsilon^n$$

have a convergence radius bounded below by $\varepsilon_R = \frac{1}{C_1^2}$ on $\Omega \setminus \sigma$. Thus, this implies the convergence of this series if $\varepsilon > 0$ and $\varepsilon < \varepsilon_R$. It is straightforward to extend the convergence to $\varepsilon = 0$.

Now we have to prove that the sum of this series is u_ε. By summing the various problems $(\tilde{\mathcal{P}}_n)$ with appropriate coefficients (equal to ε^n), and by dividing the equation in $\Omega \setminus \sigma$ in (37) by ε, we obtain the following problem

$$\begin{cases} -\dfrac{1}{\varepsilon}\mathrm{div}(\nabla u_0) + \displaystyle\sum_{n=0}^{\infty} \varepsilon^n(-\mathrm{div}(\nabla u_{n+1}) + u_n) = v & \text{in } \Omega \setminus \sigma, \\ \displaystyle\sum_{n=0}^{\infty} \varepsilon^n \partial_n u_n = 0 & \text{on } \sigma, \\ \displaystyle\sum_{n=0}^{\infty} \varepsilon^n \partial_n u_n = 0 & \text{on } \partial\Omega, \end{cases}$$

as the various series are convergent. This problem can be rewritten as follows

$$\begin{cases} -\mathrm{div}\left(\dfrac{1}{\varepsilon}\displaystyle\sum_{n=0}^{\infty}\varepsilon^n u_n\right)+\displaystyle\sum_{n=0}^{\infty}\varepsilon^n u_n = v & \text{in } \Omega\setminus\sigma,\\ \partial_n\left(\displaystyle\sum_{n=0}^{\infty}\varepsilon^n u_n\right)=0 & \text{on } \sigma,\\ \partial_n\left(\displaystyle\sum_{n=0}^{\infty}\varepsilon^n u_n\right)=0 & \text{on } \partial\Omega. \end{cases}$$

One can then see that the function of $H^1(\Omega\setminus\sigma)$ equal to $\sum_{n=0}^{\infty}u_n\varepsilon^n$ is the solution to problem $(\tilde{\mathcal{P}}_\varepsilon)$, and thus is equal to u_ε by uniqueness of the solution. □

3.4. Quadrature formula and approximation of u_0

We recall that it is possible to numerically compute u_ε for not too small values of $\varepsilon > 0$, and the goal is to compute u_0. We can define a function of $\varepsilon\in\mathbb{R}^+$ as follows

$$f(\varepsilon) := u_\varepsilon \in H^1(\Omega\setminus\sigma). \tag{42}$$

From the previous theorem, we know that f has a power series expansion at the origin

$$f(\varepsilon)=\sum_{n=0}^{\infty}u_n\varepsilon^n, \tag{43}$$

which is valid for $0\le\varepsilon<\varepsilon_R$. We denote by $\varepsilon_c>0$ the smallest value of ε for which it is easy to numerically compute $f(\varepsilon)$. From a numerical point of view, it is clear that $\varepsilon_c\ll 1$ and then we can assume that $\varepsilon_c\ll\varepsilon_R$. We can then use in the following any $f(\varepsilon)$ for $0<\varepsilon_c\le\varepsilon<\varepsilon_R$. It is also possible to assume, without any restriction, that ε_R is strictly smaller than the convergence radius.

We will now construct an approximation $\tilde{u}_0$ of u_0. We first choose N points $(\varepsilon_i)_{i=1\dots N}$ in $[\varepsilon_c,\varepsilon_R]$, and compute the corresponding values $(f(\varepsilon_i))_{i=1\dots N}$. We can compute an interpolation polynomial g_N of degree $N-1$ defined by

$$g_N(\varepsilon)=\sum_{i=1}^{N}\left(\prod_{j=1,j\neq i}^{N}\frac{\varepsilon-\varepsilon_j}{\varepsilon_i-\varepsilon_j}\right)u_{\varepsilon_i}. \tag{44}$$

We define $\varepsilon_m=\max_{i=1\dots N}\varepsilon_i$. The interpolation error is then given by

$$f(0)-g_N(0)=\frac{(-1)^N f^{(N)}(\varepsilon)}{N!}\prod_{i=1}^{N}\varepsilon_i, \tag{45}$$

where $\varepsilon\in[0,\varepsilon_m]$.

In the particular case where $\varepsilon_i=i\varepsilon_c$, if we assume that N is smaller than $\frac{\varepsilon_R}{\varepsilon_c}$, then

$$|f(0)-g_N(0)|=f^{(N)}(\varepsilon)\,\varepsilon_c^N, \tag{46}$$

for a particular $\varepsilon\in[0,N\varepsilon_c]$. As all derivatives of f have the same convergence radius, then $\|f^{(N)}\|_{H^1(\Omega\setminus\sigma)}$ has a finite maximum value on $[0,N\varepsilon_c]$, which we denote by M. If we define $\tilde{u}_0=g_N(0)$, then

$$\|u_0-\tilde{u}_0\|_{H^1(\Omega\setminus\sigma)}\le M\,\varepsilon_c^N. \tag{47}$$

If we choose $N=1$, the approximation is simply $\tilde{u}_0=f(\varepsilon_c)$, and the approximation error is $\mathcal{O}(\varepsilon_c)$. For $N=2$, the approximation error is $\mathcal{O}({\varepsilon_c}^2)$.

3.5. Segmentation algorithm

We can then define a segmentation algorithm:

- Solve the direct and adjoint equations of the restoration problem with $c=c_0\sim 1$ everywhere:

$$\begin{cases} -\mathrm{div}\,(c_0\nabla u)+u=v & \text{in } \Omega,\\ \partial_n u=0 & \text{on } \partial\Omega, \end{cases} \tag{48}$$

$$\begin{cases} -\mathrm{div}(c_0\nabla p)+p=-\partial_u J(u) & \text{in } \Omega,\\ \partial_n p=0 & \text{on } \partial\Omega, \end{cases} \tag{49}$$

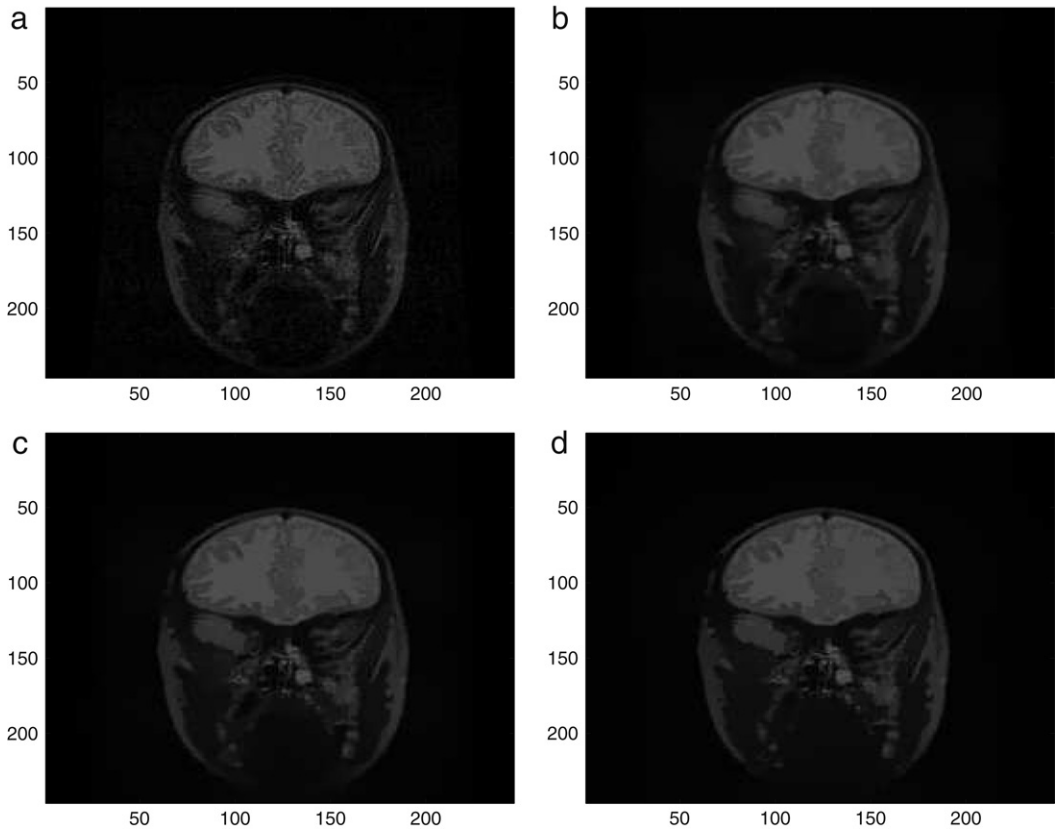

Fig. 4. Segmentation of a medical image: initial image (256 × 256 pixels) (a); Solutions of problem $(\tilde{\mathcal{P}}_\varepsilon)$ for $\varepsilon = 10^{-1}$ (b), $\varepsilon = 10^{-2}$ (c) and $\varepsilon = 10^{-3}$ (d).

where the cost function J is defined by

$$J(u) = \int_\Omega \|\nabla u\|^2. \tag{50}$$

- Compute the 2×2 matrix M defined by

$$M(x) = -\pi c_0 \frac{\nabla u(x) \nabla p(x)^{\mathrm{T}} + \nabla p(x) \nabla u(x)^{\mathrm{T}}}{2} - \pi \nabla u(x) \nabla u(x)^{\mathrm{T}}, \tag{51}$$

and its lowest eigenvalue $\lambda_{\min}$ at each point of the domain Ω.
- Set

$$\sigma = \{x \in \Omega;\ \lambda_{\min} < \alpha < 0\} \tag{52}$$

where α is a small negative threshold.
- Set $\varepsilon_c > 0$ to the minimal value of ε for which it is easy to compute numerically the solution u_ε of problem $(\tilde{\mathcal{P}}_\varepsilon)$ defined by Eq. (32).
- Choose $N \in \mathbb{N}^*$ in order to have an approximation error in $\mathcal{O}(\varepsilon_c{}^N)$.
- Compute the solutions $(u_{i\varepsilon_c})_{i=1\ldots N}$ in $H^1(\Omega \setminus \sigma)$ of problems $(\tilde{\mathcal{P}}_{i\varepsilon_c})$ defined by

$$(\tilde{\mathcal{P}}_{i\varepsilon_c}) \begin{cases} -\mathrm{div}\left(\dfrac{1}{i\varepsilon_c} \nabla u_{i\varepsilon_c}\right) + u_{i\varepsilon_c} = v & \text{in } \Omega \setminus \sigma, \\ \partial_n u_{i\varepsilon_c} = 0 & \text{on } \sigma, \\ \partial_n u_{i\varepsilon_c} = 0 & \text{on } \partial\Omega, \end{cases} \tag{53}$$

for $i = 1 \ldots N$.
- Compute the interpolation polynomial g_N of degree $N - 1$ for $\varepsilon = 0$

$$\tilde{u}_0 = g_N(0) = \sum_{i=1}^{N} \left(\prod_{j=1, j\neq i}^{N} \frac{j}{j-i} \right) u_{i\varepsilon_c}. \tag{54}$$

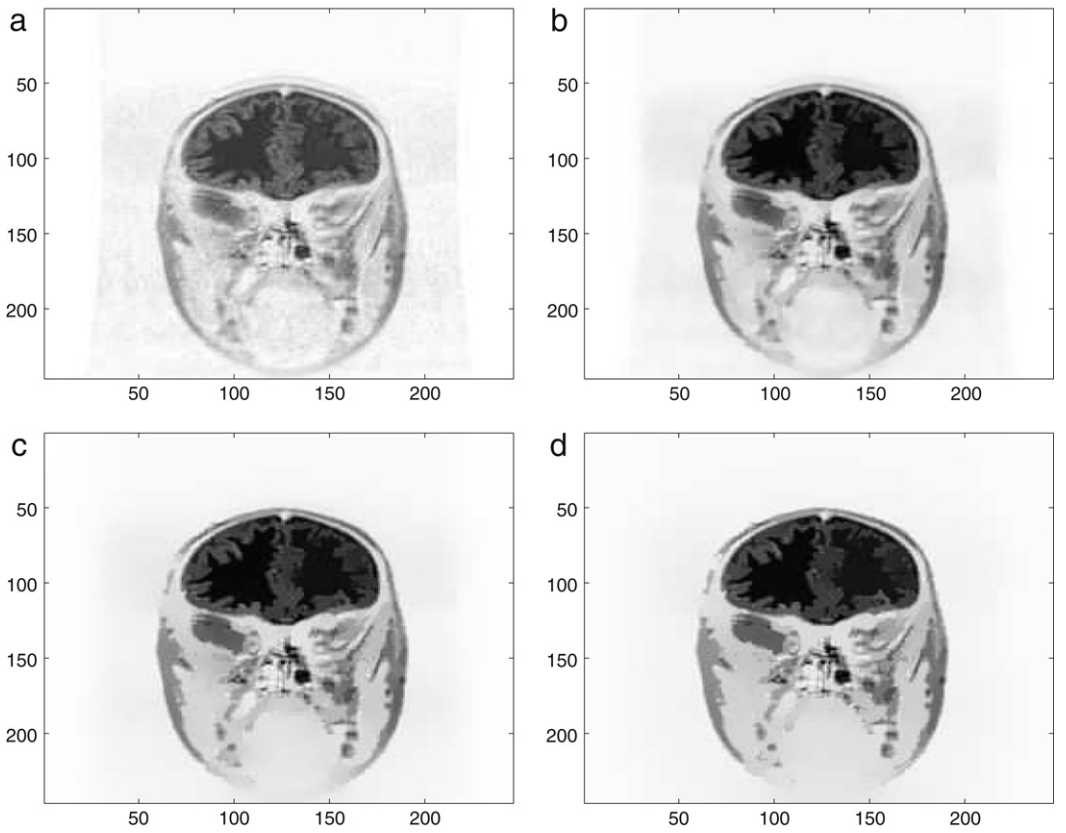

Fig. 5. Segmentation of a medical image, using a different scale for the displaying of images: initial image (256 × 256 pixels) (a); Solutions of problem $(\tilde{\mathcal{P}}_\varepsilon)$ for $\varepsilon = 10^{-1}$ (b), $\varepsilon = 10^{-2}$ (c) and $\varepsilon = 10^{-3}$ (d).

- $\tilde{u}_0$ is an approximation of the segmented image u_0 satisfying

$$\|u_0 - \tilde{u}_0\|_{H^1(\Omega\setminus\sigma)} = \mathcal{O}(\varepsilon_c^N). \tag{55}$$

This algorithm has a complexity in $\mathcal{O}(N.n.\log(n))$ where n is the number of pixels in the image, and N is the degree of the interpolation approximation (see Section 2 and [7,8] for more details). In numerical experiments, N will be of the order of 1, typically $2 \leq N \leq 5$.

3.6. Numerical results

We first present the numerical solutions of problem $(\tilde{\mathcal{P}}_\varepsilon)$ defined by Eq. (32), for several values of ε, from 10^{-1} to 10^{-3}. It was not possible to compute the solution for $\varepsilon = 10^{-4}$, as the preconditioned conjugate gradient algorithm was unable to converge in a reasonable number of iterations. These results are presented in Fig. 4. One can see that the image converges towards a piecewise constant function as ε decreases, but some edges are also degraded as ε goes to zero. This is mainly due to the fact that the resolution of problem $(\tilde{\mathcal{P}}_\varepsilon)$ needs a quite large number of conjugate gradient iterations for a small value of ε, and the computed solution is not satisfying.

Fig. 5 shows the same results, but with a different grey scale (only for displaying, not for solving the equation) in order to have a better view of the different images.

Fig. 6 shows the solution of problem $(\tilde{\mathcal{P}}_\varepsilon)$ defined by Eq. (32), for $\varepsilon = 10^{-1}$, and the corresponding interpolated solution (see Eq. (54)) for $\varepsilon_c = 10^{-1}$ and $N = 5$. On the bottom of the same figure are presented the solution of the same problem for $\varepsilon = 10^{-2}$ and the interpolated solution corresponding to $\varepsilon_c = 10^{-2}$ and $N = 5$. Visually, the images are quite similar. In order to have a better view of the quality of the images, and particularly the discrepancy to a piecewise constant function outside the edges, we have computed the gradient (outside the edges) of these images.

Fig. 7 shows the L^2 norm of the gradient of the interpolated solution on $\Omega \setminus \sigma$ versus the computational cost for several values of N (on each curve, from $N = 1$ (left) to $N = 10$ (right) every 1) and ε_c (5 curves corresponding to $\varepsilon_c = 10^{-1}$, 3.10^{-2}, and 10^{-2}). One can see that once ε_c is chosen, it is possible to get a much more precise approximation of u_0 while multiplying by less than 2 or 3 the computational cost by using our segmentation algorithm (see the previous section). The approximation error can be nearly divided by 2 by using the solutions corresponding to several multiples of ε_c. The most

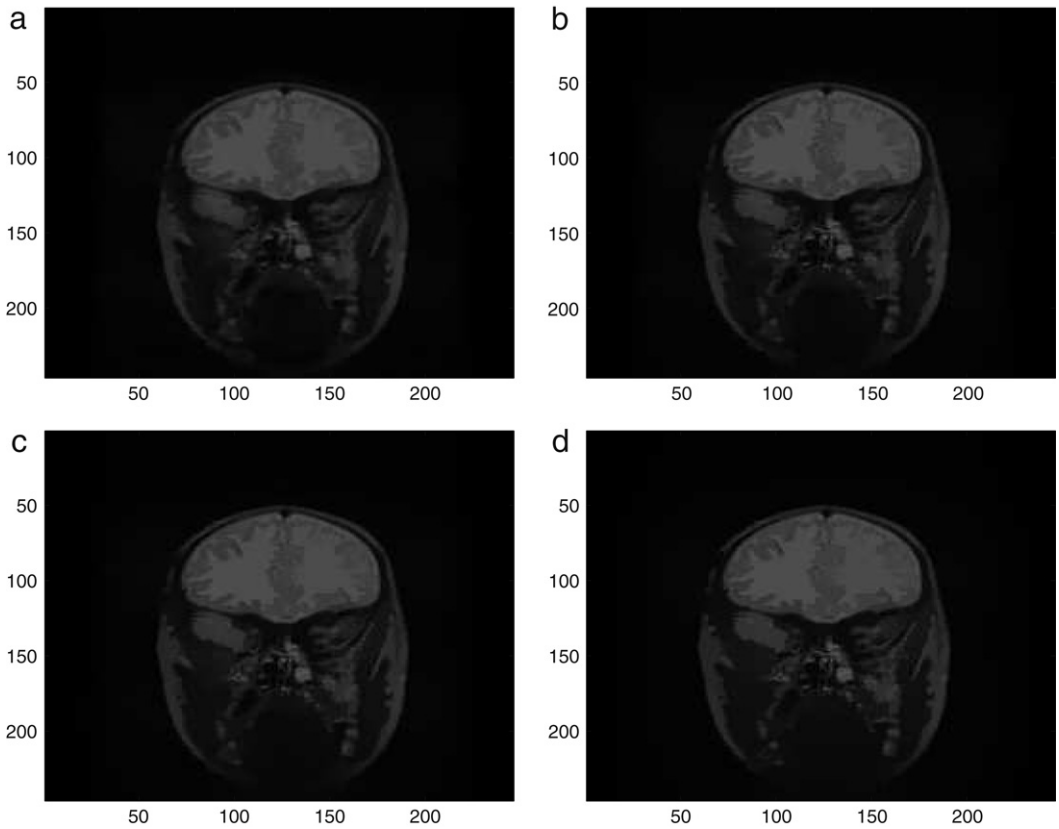

Fig. 6. Segmentation of a medical image: Solution of problem $(\tilde{\mathcal{P}}_\varepsilon)$ for $\varepsilon = 10^{-1}$ (a); interpolated solution of problem $(\tilde{\mathcal{P}}_\varepsilon)$ for $\varepsilon = 10^{-1}$ and $N = 5$ (b); (c) and (d): same as (a) and (b) for $\varepsilon = 10^{-2}$.

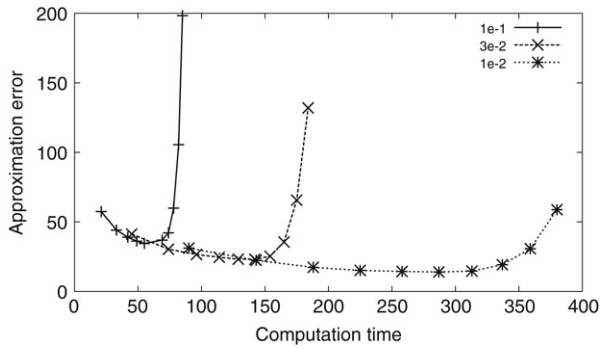

Fig. 7. Segmentation of a medical image: norm of the gradient of the interpolated solution on $\Omega \setminus \sigma$ for $N = 1 \ldots 10$ (10 points on a same curve) versus the computational cost, for several values of ε_c: 10^{-1}, 3.10^{-2}, and 10^{-2} (3 curves).

interesting point is that it is possible to compute faster a better solution using a larger value of ε_c and some of its multiples with our algorithm than computing directly the solution of problem $\tilde{\mathcal{P}}_\varepsilon$ for a smaller value of ε directly. Moreover, we have seen that it may be impossible to compute directly this solution for a too small value of ε.

We can also see that the solution is degraded when using a large N (larger than 6 or 7). This is mainly due to the fact that the interpolation scheme is centered, and for $N = 10$ for example, the solution corresponding to $\varepsilon = 5\varepsilon_c$ has a much larger coefficient than the solution corresponding to $\varepsilon = \varepsilon_c$, and $N\varepsilon_c$ may be larger than the convergence radius of the power series. Finally, the optimal value for N is between 3 and 6 in the sense that the smaller gradient corresponds to nearly $N = 6$, but the larger gradient decreasing to time consuming ratio corresponds to smaller values of N, nearly $N = 3$.

4. Conclusion

We recalled in the first part of this paper a restoration process for medical images based on the topological asymptotic analysis. We presented then an extension to the image segmentation problem by considering the restoration process, with

different values of the conductivity coefficient. It is indeed possible to explicitly rewrite the solution of an approximate segmentation problem for asymptotically small values of the conductivity coefficient as a power series expansion with respect to this coefficient. The computation of several approximations (corresponding to quite large conductivity coefficients) of the segmented image allows us to obtain a very good approximation of the segmented image, which is much more precise than a directly computed solution corresponding to a very small conductivity. The numerical computation of the solution for very small conductivities is faster and more precise with our segmentation approach than using a direct resolution approach.

A future work is to study the natural extension of this work to 3D images, or movies, as a 3D segmentation directly provides a full spatial information whereas a 2D segmentation of each slice of the 3D image requires some post-processing.

References

[1] G. Alessandrini, A. Diaz Valenzuela, Unique determination of multiple cracks by two measurements, SIAM J. Control Optim. 34 (3) (1996) 913–921.
[2] H. Ammari, M.S. Vogelius, D. Volkov, Asymptotic formulas for perturbations in the electromagnetic fields due to the presence of inhomogeneities of small diameter II - The full Maxwell equations, J. Math. Pure Appl. 80 (8) (2001) 769–814.
[3] S. Amstutz, I. Horchani, M. Masmoudi, Crack detection by the topological gradient method, Control Cybern. 34 (1) (2005) 119–138.
[4] S. Amstutz, M. Masmoudi, B. Samet, The topological asymptotic for the Helmoltz equation, SIAM J. Control Optim. 42 (5) (2003) 1523–1544.
[5] S. Andrieux, A. Ben Abda, Identification of planar cracks by complete overdetermined data: Inversion formulae, Inverse Problems 12 (1996) 553–563.
[6] G. Aubert, P. Kornprobst, Mathematical Problems in Image Processing, in: Applied Mathematical Sciences, vol. 147, Springer-Verlag, 2001.
[7] D. Auroux, L. Jaafar Belaid, M. Masmoudi, A topological asymptotic analysis for the regularized grey-level image classification problem, Math. Model. Numer. Anal. 41 (3) (2007) 607–625.
[8] D. Auroux, M. Masmoudi, A one-shot inpainting algorithm based on the topological asymptotic analysis, Comput. Appl. Math. 25 (2–3) (2006) 1–17.
[9] Z. Belhachmi, D. Bucur, Stability and uniqueness for the crack identification problem, SIAM J. Control Optim. 46 (1) (2007) 253–273.
[10] A. Ben Abda, H. Ben Ameur, M. Jaoua, Identification of 2D cracks by elastic boundary measurements, Inverse Problems 15 (1999) 67–77.
[11] A. Ben Abda, M. Kallel, J. Leblond, J.-P. Marmorat, Line-segment cracks recovery from incomplete boundary data, Inverse Problems 18 (2002) 1057–1077.
[12] A. Blake, M. Isard, Active Contours, Springer-Verlag, 1998.
[13] M. Bruhl, M. Hanke, M. Pidcock, Crack detection using electrostatic measurements, Math. Model. Numer. Anal. 35 (2001) 595–605.
[14] K. Bryan, M.S. Vogelius, A review of selected works on crack identification, in: Proceedings of the IMA workshop on Geometric Methods in Inverse Problems and PDE Control, August 2001.
[15] A.P. Calderón, On an inverse boundary value problem, in: Seminar on Numerical Analysis and its Applications to Continuum Physics (Rio de Janeiro, 1980), Soc. Brasil. Mat., Rio de Janeiro, Brasil, 1980, pp. 65–73.
[16] F. Catté, T. Coll, P.L. Lions, J.M. Morel, Image selective smoothing and edge detection by non linear diffusion, SIAM J. Numer. Anal. 29 (1992) 182–193.
[17] J.S. Duncan, N. Ayache, Medical image analysis: Progress over two decades and the challenges ahead, IEEE Trans. Pattern Anal. Mach. Intell. 22 (1) (2000) 85–106.
[18] A. Friedman, M.S. Vogelius, Determining cracks by boundary measurements, Indiana Univ. Math. J. 38 (3) (1989) 527–556.
[19] A. Friedman, M.S. Vogelius, Identification of small inhomogeneities of extreme conductivity by boundary measurements: A theorem of continuous dependence, Arch. Ration. Mech. Anal. 105 (4) (1989) 299–326.
[20] S. Garreau, P. Guillaume, M. Masmoudi, The topological asymptotic for PDE systems: The elasticity case, SIAM J. Control Optim. 39 (6) (2001) 1756–1778.
[21] P. Guillaume, M. Masmoudi, A. Zeglaoui, From compressible to incompressible materials via an asymptotic expansion, Numer. Math. 91 (2002) 649–673.
[22] P. Guillaume, K. Sididris, The topological asymptotic expansion for the Dirichlet problem, SIAM J. Control Optim. 41 (4) (2002) 1042–1072.
[23] P. Guillaume, K. Sididris, The topological sensitivity and shape optimization for the Stokes equations, SIAM J. Control Optim. 43 (1) (2004) 1–31.
[24] L. Jaafar Belaid, M. Jaoua, M. Masmoudi, L. Siala, Image restoration and edge detection by topological asymptotic expansion, C. R. Acad. Sci. Sér. I 342 (55) (2006) 313–318.
[25] L. Jaafar Belaid, M. Jaoua, M. Masmoudi, L. Siala, Application of the topological gradient to image restoration and edge detection, Eng. Anal. Bound. Elem. (2008) (in press).
[26] R. Kohn, M. Vogelius, Relaxation of a variational method for impedance computed tomography, Commun. Pure Appl. Math. 40 (6) (1987) 745–777.
[27] S. Kubo, K. Ohji, Inverse problems and the electric potential computed tomography method as one of their application, in: Mechanical Modeling of New Electromagnetic Materials, Elsevier Science Publisher, 1990.
[28] M. Masmoudi, The topological asymptotic, Computational Methods for Control Applications, in: R. Glowinski, H. Karawada, J. Periaux (Eds.), GAKUTO Internat. Ser. Math. Sci. Appl. vol. 16, Tokyo, Japan, 2001, pp. 53–72.
[29] T. McInerney, D. Terzopoulos, Medical image segmentation using topologically adaptable surfaces, in: Proc. CVRMed'97, Grenoble, France, 1997.
[30] D. Mumford, J. Shah, Optimal approximations by piecewise smooth functions and associated variational problems, Commun. Pure Appl. Math. 42 (5) (1989) 577–685.
[31] N. Nishimura, S. Kobayashi, A boundary integral equation method for an inverse problem related to crack detection, Internat. J. Numer. Methods Engrg. 32 (1991) 1371–1387.
[32] P. Perona, J. Malik, Scale space and Edge detection detection using Anisotropic diffusion, IEEE Trans. Pattern Analy. Mach. Intell. 12 (1990) 629–639.
[33] D.L. Pham, C. Xu, J.L. Prince, A survey of current methods in medical image segmentation, Tech. Report Johns Hopkins Univ., JHU/ECE 99-01 (1999).
[34] B. Samet, S. Amstutz, M. Masmoudi, The topological asymptotic for the helmholtz equation, SIAM J. Control Optim. 42 (5) (2003) 1523–1544.
[35] F. Santosa, M. Vogelius, A computational algorithm to determine cracks from electrostatic boundary measurements, Internat. J. Engrg. Sci. 29 (1991) 917–937.
[36] J.A. Sethian, Level set methods and fast marching methods: Evolving interfaces in computational geometry, fluid mechanics, computer vision, and materials sciences, in: Cambridge Monograph on Applied and Computational Mathematics, Cambridge University Press, Cambridge, 1999.
[37] J. Sokolowski, A. Zochowski, Topological derivatives of shape functionals for elasticity systems, Internat. Ser. Numer. Math 139 (2002) 231–244.
[38] M. Wei, A fast snake model based on non-linear diffusion for medical image segmentation, Comput. Med. Imaging Graph. 28 (3) (2004) 109–117.
[39] J. Weickert, Theoretical foundations of anisotropic diffusion in image processing, Computing, Suppl. 11 (1996) 221–236.
[40] J. Weickert, Anisotropic diffusion in image processing, Ph.D. Thesis, University of Kaiserslautern, Germany, 1996.
[41] J. Weickert, Efficient image segmentation using partial differential equations and morphology, Pattern Recognit. 34 (9) (2001) 1813–1824.
[42] A. Yezzi, S. Kichenassamy, A. Kumar, P. Olver, A. Tannenbaum, A Geometric Snake Model for Segmentation of Medical Imagery, IEEE Trans. Med. Imaging 16 (2) (1997) 199–209.